

Higher-Order Non-Oscillatory Schemes in Ideal Magnetohydrodynamics

Debojyoti Ghosh* Avijit Chatterjee†

Department of Aerospace Engineering,
Indian Institute of Technology Bombay
Mumbai 400076, India

Abstract

In recent years, there has been a growing interest in the numerical solution of the MHD system, particularly the idealized system, which is obtained by neglecting dissipative effects. High-resolution schemes, which were successfully applied to the Euler equations, have been tried for the MHD equations. The non-convexity and coincidence of eigenvalues for some cases raises additional questions regarding the convergence of numerical schemes. In the present paper, the 1st order upwind, 2nd and 3rd order Essentially Non-Oscillatory and 5th order Weighted Essentially Non-Oscillatory schemes have been used on the 1D ideal MHD equations. A characteristic-based is used where the flux vector is resolved along the characteristic directions and reconstructed in an upwind manner. Results are presented for the MHD shock tube and the high Mach number test cases.

Keywords: Ideal Magnetohydrodynamics, ENO, WENO, characteristics, high-resolution schemes

1 Introduction

Magnetohydrodynamics is a combination of fluid mechanics and electromagnetics. It describes the behavior of an electrically conducting fluid in the presence of electric and magnetic fields. Its applications are largely in the areas of astrophysics (flow of interstellar gas masses, interaction of solar winds with the planetary magnetic field, etc). In recent times, it has become important in the context of hypersonic vehicles where the temperatures are high enough to ionize the surrounding gases. Technologies for using the properties of plasma for drag reduction and stealth have been recently considered. In view of all this, there has been a growing interest in the numerical solution of the magnetohydrodynamic (MHD) equations.

The idealized MHD equations are derived from the complete equations by neglecting dissipative terms like viscosity, heat conduction and electrical resistivity of the gases [1]. The ideal MHD equations form a non-strictly hyperbolic system where, upto five, out of the seven eigenvalues can coincide. It has also been shown that these equations are non-convex [2], thus allowing for the formation of compound waves, e.g. consisting of a rarefaction wave attached to a shock of the same family. These properties prevent the straightforward application of Godunov-type algorithms developed for the Euler equations to the MHD system. Many issues, especially the question of shock admissibility, are yet to be resolved [3].

Following the successful application of high resolution upwind schemes to the Euler equations, these have also been applied to the MHD system. Brio and Wu [2] introduced an upwind differencing scheme which was based on a Roe-type approximate Riemann solver. The drawback of their scheme was that a Roe averaged Jacobian could not be found except in the case $\gamma = 2$. Later, Cargo and Gallice [4] outlined the construction of Roe matrices for the ideal MHD for the general case. Zachary and Collela [5] have considered a modification of the Engquist - Osher flux while Toth and Odstrcil [6]

*Under-graduate student, Email: ghosh@aero.iitb.ac.in, Phone: +91-22-25720011

†Assoc. Professor (Corresponding Author), Email: avijit@aero.iitb.ac.in, Phone: +91-22-25767128

have compared some FCT and TVD schemes for the MHD Riemann problem. Khanfir [7] introduced an extension of the kinetic schemes to the MHD system.

The Essentially Non-Oscillatory (ENO) and Weighted Essentially Non-Oscillatory (WENO) family of schemes have been applied to the Euler equations as well as the equations of electromagnetics with excellent results. Previous attempts have been made to apply the flux-differencing form of the WENO schemes to the 1D MHD system [12, 16] and the results are encouraging. In the present paper, the ENO and WENO schemes have been applied to equations of ideal 1D MHD and the performance of these high-resolution schemes are compared for the two coplanar MHD Riemann problems formulated in [2]. A characteristic based algorithm has been developed which decomposes the flux vector into its component along each of the seven characteristic directions. These components are reconstructed using the ENO/WENO schemes and upwinding is done based on the sign of the corresponding eigenvalue. This is a straightforward application of the approach used for the Euler equations to the MHD system and thus suffers from the drawback of non-unique structure of intermediate shocks. It may be possible to solve this problem by using dissipative terms modeling the actual physical dissipation while capturing intermediate shocks. However, these problems are not faced in the present study since both the test cases are coplanar problems with a unique intermediate shock structure. The first test case is an extension of Sod's shock tube test for the Euler equations and the solution contains a compound wave consisting of an intermediate shock attached to a slow rarefaction wave, apart from a regular slow shock, fast rarefaction waves and a contact discontinuity. The second test case is high Mach number problem, where Mach numbers go upto 15.5 and tests the robustness of the schemes. It can be formulated as a standard hydrodynamical problem with full pressure being equivalent to the gas pressure, and thus the analytical result can be found. It should also be mentioned that in the absence of magnetic field, the MHD equations reduce to the Euler equations and thus the standard hydrodynamical problems used to validate Euler solvers (like Sod's test) can be used here as well. The results computed by the higher order non-oscillatory schemes are compared with the first order upwind scheme and with results presented in [2, 5, 4, 6, 12].

The layout of the paper is as follows. In section 2, the MHD equations and their 1D form are defined. A brief description of the MHD eigenstructure for the 1D case is also given. The eigenvalues and a complete set of well-defined eigenvectors, which are essential to our characteristic-based algorithm, have been presented. Section 3 gives an outline of our numerical treatment of the equations. The 1st order upwind, 2nd and 3rd order ENO and 5th order WENO schemes have been used to solve for the two test cases. Section 4 presents the results thus obtained.

2 Governing Equation

The ideal MHD equations govern the behavior of a conducting fluid in the presence of a magnetic field, neglecting dissipative effects like viscosity, heat conduction and electrical resistivity. They are an extension of the Euler equations including terms representing electromagnetic momentum and energy. Additionally, there is an equation governing the evolution of the magnetic field. Using units such that factors like $4\pi, \mu_0$ and c do not appear, the ideal MHD system can be obtained as [1, 2]:

$$\rho_t + \nabla \cdot (\rho u) = 0 \quad (1)$$

$$(\rho u)_t + \nabla \cdot (\rho uu + \gamma P^* \mathbf{I} - \mathbf{B}\mathbf{B}) = 0 \quad (2)$$

$$\mathbf{B}_t + \nabla \cdot (\mathbf{uB} - \mathbf{Bu}) = 0 \quad (3)$$

$$\mathbf{E}_t + \nabla \cdot ((E + P^*) \mathbf{u} - (\mathbf{u} \cdot \mathbf{B}) \mathbf{B}) = 0 \quad (4)$$

where $P^* = P + \mathbf{B} \cdot \mathbf{B}/2$ is the full pressure (defined as the sum of gas pressure and the magnetic pressure) and $E = \rho u \cdot u/2 + P/(\gamma - 1) + \mathbf{B} \cdot \mathbf{B}/2$ is the total energy of the system. Additionally, the divergence free condition $\nabla \cdot \mathbf{B} = 0$ needs to be satisfied. Theoretically, if the initial conditions satisfy this constraint, then the solution at all time satisfies it. However, in numerical computations, small errors can arise which causes non-zero divergence of the magnetic field. These considerations are important while solving multi-dimensional problems.

The 1D system can be obtained by assuming that the gradients exist only along the x-direction. The resulting system can be written in conservative form as:

$$\mathbf{U}_t + \mathbf{F}(\mathbf{U})_x = 0 \quad (5)$$

where \mathbf{U} is the conserved vector and $\mathbf{F}(\mathbf{U})$ is the flux vector.

$$\mathbf{U} = \begin{bmatrix} \rho \\ \rho u \\ \rho v \\ \rho w \\ B_y \\ B_z \\ E \end{bmatrix}, \quad \mathbf{F}(\mathbf{U}) = \begin{bmatrix} \rho u \\ \rho u^2 + P^* \\ \rho uv - B_y B_z \\ \rho uw - B_z B_x \\ u B_y - v B_z \\ u B_z - w B_x \\ (E + P^*)u - B_z(u B_z + v B_y + w B_x) \end{bmatrix} \quad (6)$$

In 1D, the zero divergence constraint results in the condition $B_z = \text{constant}$ which is satisfied by the above system.

Eigenstructure

The above system, equation (5), is hyperbolic in nature, with seven eigenvalues and a complete set of eigenvectors. It is not a strictly hyperbolic system since five out of seven eigenvalues can coincide. The wave structure of this system is given by the seven waves:

- Entropy wave with wavespeed u
- two Alfvén waves with wavespeeds $u \pm c_a$
- two fast magnetosonic waves with wavespeeds $u \pm c_f$
- two slow magnetosonic waves with wavespeeds $u \pm c_s$

where

$$c_a = B_z / \sqrt{\rho} \quad (7)$$

$$c_{f,s}^2 = \frac{1}{2} \left[\frac{\gamma P + B \cdot B}{\rho} \pm \sqrt{\left(\frac{\gamma P + B \cdot B}{\rho} \right)^2 - \frac{4\gamma PB_z^2}{\rho}} \right] \quad (8)$$

These eigenvalues can coincide for two cases:

- $B_z = 0$: In this case, the Alfvén and slow wavespeeds coincide with the entropy wave and thus u is an eigenvalue with multiplicity 5. The problem becomes equivalent to a aerodynamic problem if the gas pressure is replaced with the full pressure. The fast magnetosonic wavespeed is equivalent to the speed of sound.
- $B_y^2 + B_z^2 = 0$: In this case, $c_f^2 = \max(a^2, c_a^2)$ and $c_s^2 = \min(a^2, c_a^2)$ where a is the speed of sound ($a = \sqrt{\gamma P / \rho}$). Thus, for $a^2 \neq c_a^2$, the eigenvalues $u \pm c_a$ are of multiplicities 2. Additionally, if $a^2 = c_a^2$, then the multiplicities of $u \pm c_a$ is 3. This point has been referred to as the "triple umbilic" in [8].

The eigenvectors for this system, proposed in [13], were incomplete and became singular near these cases. Brio and Wu [2] used a renormalization process to ensure that their set of eigenvectors were well-defined at all points. Presently, two different eigenstructures exist for this system. One has been proposed by Roe and Balsara [8] and is derived from the governing equations written in terms of primitive variables. The other has been proposed by Ryu and Jones [14] and is derived from the governing equations written in terms of the conserved variables. It has been reported [15] that though both yield the same result in 1D, the Ryu and Jones eigenstructure is unstable leading to negative pressures and densities in multi-dimensional problems. In the present study, Roe and Balsara's eigenstructure has been used.

The left and right eigenvectors proposed by Roe and Balsara [8] are given as follows:

$$\mathbf{r}_f^\pm = \begin{bmatrix} \alpha_f \rho \\ \pm \alpha_f c_f \\ \mp \alpha_s c_s \beta_y \text{sgn}(B_z) \\ \mp \alpha_s c_s \beta_z \text{sgn}(B_z) \\ \alpha_s \sqrt{4\pi \rho a \beta_y} \\ \alpha_s \sqrt{4\pi \rho a \beta_z} \\ \alpha_f \rho a^2 \end{bmatrix}, \quad \mathbf{l}_f^\pm = \frac{1}{2a^2} \begin{bmatrix} 0 \\ \pm \alpha_f c_f \\ \mp \alpha_s c_s \beta_y \text{sgn}(B_z) \\ \mp \alpha_s c_s \beta_z \text{sgn}(B_z) \\ a_s a \beta_y / \sqrt{4\pi \rho} \\ a_s a \beta_z / \sqrt{4\pi \rho} \\ \alpha_f / \rho \end{bmatrix} \quad (9)$$

$$r_s^\pm = \begin{bmatrix} \alpha_s \rho \\ \pm \alpha_s c_s \\ \pm \alpha_f c_f \beta_y \operatorname{sgn}(B_z) \\ \pm \alpha_f c_f \beta_z \operatorname{sgn}(B_z) \\ -\alpha_f \sqrt{4\pi \rho a} \beta_y \\ -\alpha_f \sqrt{4\pi \rho a} \beta_z \\ a_s \rho a^2 \end{bmatrix}, l_s^\pm = \frac{1}{2a^2} \begin{bmatrix} 0 \\ \pm \alpha_s c_s \\ \pm \alpha_f c_f \beta_y \operatorname{sgn}(B_z) \\ \pm \alpha_f c_f \beta_z \operatorname{sgn}(B_z) \\ -\alpha_f a \beta_y / \sqrt{4\pi \rho} \\ -\alpha_f a \beta_z / \sqrt{4\pi \rho} \\ a_s / \rho a \end{bmatrix} \quad (10)$$

$$r_a^\pm = \begin{bmatrix} 0 \\ 0 \\ \pm \beta_z \\ \mp \beta_y \\ -\sqrt{4\pi \rho \beta_z} \operatorname{sgn}(B_z) \\ \sqrt{4\pi \rho \beta_y} \operatorname{sgn}(B_z) \\ 0 \end{bmatrix}, l_a^\pm = \frac{1}{2} \begin{bmatrix} 0 \\ 0 \\ \pm \beta_z \\ \mp \beta_y \\ -\beta_z \operatorname{sgn}(B_z) \\ \sqrt{4\pi \rho} \\ \beta_y \operatorname{sgn}(B_z) \\ \sqrt{4\pi \rho} \end{bmatrix}, r_a = \begin{bmatrix} 1 \\ 0 \\ 0 \\ 0 \\ 0 \\ 0 \\ 0 \end{bmatrix}, l_a = \begin{bmatrix} 1 \\ 0 \\ 0 \\ 0 \\ 0 \\ 0 \\ -1/a^2 \end{bmatrix} \quad (11)$$

where the renormalization parameters are given by

$$\beta_y = \frac{B_y}{\sqrt{B_y^2 + B_z^2}}, \beta_z = \frac{B_z}{\sqrt{B_y^2 + B_z^2}}, \alpha_f^2 = \frac{a^2 - c_s^2}{c_f^2 - c_s^2}, \alpha_s^2 = \frac{c_f^2 - a^2}{c_f^2 - c_s^2} \quad (12)$$

Near the cases where the eigenvalues coincide, as mentioned above, the treatment of these parameters is the same as given in [8]. These eigenvectors are derived from the governing equations written in terms of the primitive variables ($\mathbf{W} = [\rho, u, v, w, B_y, B_z, P]^T$). To use these in a scheme based on the conservative form, given by equation (5), they need to be transformed as follows:

$$L_k = l_k \frac{\partial \mathbf{W}}{\partial \mathbf{U}}, R_k = \frac{\partial \mathbf{U}}{\partial \mathbf{W}} r_k, k = 1, \dots, 7 \quad (13)$$

where $\partial \mathbf{W} / \partial \mathbf{U}$ and $\partial \mathbf{U} / \partial \mathbf{W}$ are the Jacobians of transformation between the conserved and primitive variable spaces [15]. These matrix multiplications were carried and the final expressions were used in the code. Thus, a complete and well-defined set of orthonormal eigenvectors in the conserved variable space was obtained.

3 Numerical Scheme

The semi-discrete form of equation (5) can be written as

$$\frac{d\mathbf{U}_i}{dt} + \frac{1}{\delta x} (\mathbf{F}_{i+1/2} - \mathbf{F}_{i-1/2}) = 0 \quad (14)$$

where i is the cell index and δx is the length of a cell. A characteristic-based algorithms has been developed where the flux vector has been decomposed along the wave directions and these components have been reconstructed in an upwind fashion. The eigenvalues and the eigenvectors R_k and L_k are evaluated at an averaged state at the interface $\mathbf{U}_{avg}(U_i, U_{i+1})$. It has been shown in [2, 8] that the reconstruction does not depend on the averaged state and thus, an arithmetic mean of density, velocity, full pressure and magnetic field has been used to compute the averaged state. Depending on the sign of the eigenvalue, the starting point of the stencil for flux reconstruction has been chosen as i or $i+1$.

Four different reconstructions have been implemented: 1st order (Piecewise Constant), 2nd order ENO, 3rd order ENO and 5th order WENO. The ENO schemes fall under the class of high resolution methods developed to deal with flowfields containing discontinuities. They are able to maintain a high-order accuracy in smooth regions as well as provide non-oscillatory resolution of shocks. They have been very successfully applied to the Euler equations. The ENO schemes use adaptive stenciling to select the one with the smoothest data among all the candidate stencils. An r th order ENO scheme selects the smoothest stencil from r candidates. In the present study, the flux reconstruction version, proposed by Shu and Osher [9, 10] has been implemented because of its relative simplicity compared to the original solution reconstruction version. The ENO-Roe form [10] has been used which uses the reconstruction via primitive (RP) technique to compute the fluxes.

The ENO schemes suffer from certain drawbacks. One of them is the sensitivity of the adaptive stencilling procedure to round-off errors. Another drawback is that the selective procedure is not necessary in smooth regions and information may be lost by choosing only one stencil among the candidates and rejecting others. To overcome these problems, the WENO schemes were developed [11]. These schemes are based on using a convex combination of all the candidate stencils, instead of selecting one. The weight attached to each candidate stencil is determined based on the smoothness of data within the stencil. The weights are defined such that in smooth regions, they approach the optimal weights to achieve a higher order of accuracy, while for stencils with discontinuous data, they approach zero. Thus, an r th order ENO scheme can be modified to give a $(2r - 1)$ th order WENO scheme. In the present case, a 5th order WENO scheme has been implemented. The weights given to the three candidate stencils are as given in [12].

The semi-discrete equation (16) is advanced in time using the Runge-Kutta multi-stage time-stepping.

4 Results and Discussions

The schemes developed have been applied to two coplanar Riemann problems as described in [2]. The first case is an extension of Sod's shock tube problem and has the following initial conditions:

$$\text{Shock Tube : } \mathbf{W}_L = [1, 0, 0, 0, 1, 0, 1], \mathbf{W}_R = [0.125, 0, 0, 0, -1, 0, 0.1] \quad (15)$$

and $B_z = 0.75$ and $\gamma = 2$. The second case considered is the high Mach number problem. The initial conditions are as follows:

$$\text{High Mach No. : } \mathbf{W}_L = [1, 0, 0, 0, 1, 0, 1000], \mathbf{W}_R = [0.125, 0, 0, 0, -1, 0, 0.1] \quad (16)$$

and $B_z = 0$, $\gamma = 2$. This is equivalent to a aerodynamical Riemann problem with the full pressure being equivalent to the gas pressure. All computations are done on a grid containing 800 points and a CFL number of 0.8 for 400 time steps. The discontinuity in the initial conditions is located at the center of the computational domain. In both the cases, the computed solutions match those presented in [2, 4, 5, 6, 12].

Figures (1) to (5) show the variation of density, pressure, tangential magnetic field, normal and tangential velocities respectively for the shock tube problem for all the schemes. The solution to this problem consists of a fast rarefaction and a slow compound wave (consisting of a intermediate shock and a slow rarefaction) moving to the left and a contact discontinuity, a slow shock and a fast rarefaction wave moving to the right. In figure (1), it can be seen from the density profile that the resolution of the contact discontinuity is much sharper as the order of the scheme increases, with the 5th order WENO showing very little smearing. Figures (6) and (7) show a magnified view of the compound wave in the solution. Once again, it is seen that the higher order scheme result in considerably lesser smearing. A significant improvement in the accuracy can be observed as higher order schemes are used. However, a comparison of figure 6 with figure 9 in [2] shows no significant improvement in the numerical accuracy compared to their 2nd order scheme, having the same amount of error with respect to the analytical solution.

Figures (8) to (11) show the variation of the log of pressure, density, normal velocity and tangential magnetic field for the high Mach number problem. The Mach number corresponding to the right-moving shock wave is 15.5. Since this problem reduces to a standard hydrodynamical one with the full pressure being equivalent to the gas pressure and the fast magnetosonic wave being equivalent to the speed of sound, the analytical solution can be found [2, 12]. Once again, it is observed that the smearing over the contact discontinuity reduces considerably as higher order schemes are used (figure 11).

In both the cases considered here, it is seen that the 5th order WENO scheme produces some oscillations near the rarefaction waves as well the contact discontinuities. These oscillations are negligible in the results presented here but much more noticeable for computations on a coarser grid or lower order time-stepping. Similar oscillations have been observed in [12] and are probably caused due to the higher-order approximation.

Thus, a characteristic-based algorithm has been constructed using 1st order upwind, 2nd and 3rd order ENO and 5th order WENO reconstruction. The results indicate that the higher order

non-oscillatory schemes show considerably better resolution compared to the 1st order scheme for the MHD equations, despite some oscillations shown by the 5th order WENO. Also, the 5th order WENO scheme shows better resolution than the 2nd and 3rd order schemes. However, the schemes presented here are computationally intensive compared to schemes like Lax-Friedrich since they involve the decomposition of the flux vector into its components along the characteristic directions. The results obtained indicate the algorithms are sufficiently robust to handle loss of hyperbolicity. However, both the test cases were coplanar Riemann problems, which has an unique solution. Thus, questions regarding the admissibility of intermediate shocks in non-coplanar problems with non-unique solutions are unresolved.

References

- [1] Sutton G. W., Sherman A., 1965, "Engineering Magnetohydrodynamics", McGraw Hill, New York
- [2] Brio M., Wu C.C., 1988, "An Upwind Differencing Scheme for the Equations of Ideal Magnetohydrodynamics", Journal of Computational Physics, 75, pp. 400 - 422
- [3] Myong R.S., Roe P.L., 1998, "On Godunov-type schemes for Magnetohydrodynamics", Journal of Computational Physics, 147, pp. 545 - 567
- [4]Cargo P., Gallice G., 1997, "Roe Matrices for Ideal MHD and Systematic Construction of Roe Matrices for Systems of Conservation Laws", Journal of Computational Physics, 136, pp. 446 - 466
- [5] Zachary A.L., Colella P.A., 1992, "A Higher-Order Godunov method for the Equations of Ideal Magnetohydrodynamics", Journal of Computational Physics, 95, pp. 341 - 347
- [6] Toth G., Odstrcil D., 1996, "Comparison of Some Flux Corrected Transport and Total Variation Diminishing Numerical Schemes for Hydrodynamic and Magnetohydrodynamic Problems", Journal of Computational Physics, 128, pp. 82 - 100
- [7] Khanfir R., 1995, "Approximation volumes finis de type cinétique du système de la MHD idéale à pression isotrope", These de Doctorat, Paris XI, Paris
- [8] Roe P.L., Balsara D.S., 1996, "Notes on the Eigensystem of Magnetohydrodynamics", SIAM Journal of Applied Mathematics, 56 (1), pp. 57 - 67
- [9] Shu C.W., Osher S., 1988, "Efficient Implementation of Essentially Non-Oscillatory Shock-Capturing Schemes", Journal of Computational Physics, 77, pp. 439 - 471
- [10] Shu C.W., Osher S., 1989, "Efficient Implementation of Essentially Non-Oscillatory Shock-Capturing Schemes, II", Journal of Computational Physics, 83, pp. 32 - 78
- [11] Jiang G.S., Shu C.W., 1996, "Efficient Implementation of Weighted ENO Scheme", Journal of Computational Physics, 126, pp. 202 - 228
- [12] Jiang G.S., Shu C.W., 1999, "A High Order WENO Finite Difference Scheme for the Equations of Ideal Magnetohydrodynamics", Journal of Computational Physics, 150, pp. 561 - 594
- [13] Jeffrey A., Taniuti T., 1964, "Non-Linear Wave Propagation", Academic Press, New York
- [14] Ryu D., Jones T.W., 1995, "Numerical Magnetohydrodynamics in Astrophysics: Algorithm and Tests for One-dimensional Flow", Astrophysics Journal, 442, pp. 228 - 258
- [15] Lee D., Deane A., 2004, "A Numerical Implementation of Magnetohydrodynamics using a Staggered Mesh with High Order Godunov Fluxes", Project Final Report AMSC 663-664, University of Maryland, College Park, Maryland
- [16] Torrilhon M., Balsara D.S., 2004, "High Order WENO schemes: investigations on non-uniform convergence for MHD Riemann problems", Journal of Computational Physics, 201, pp. 586 - 600

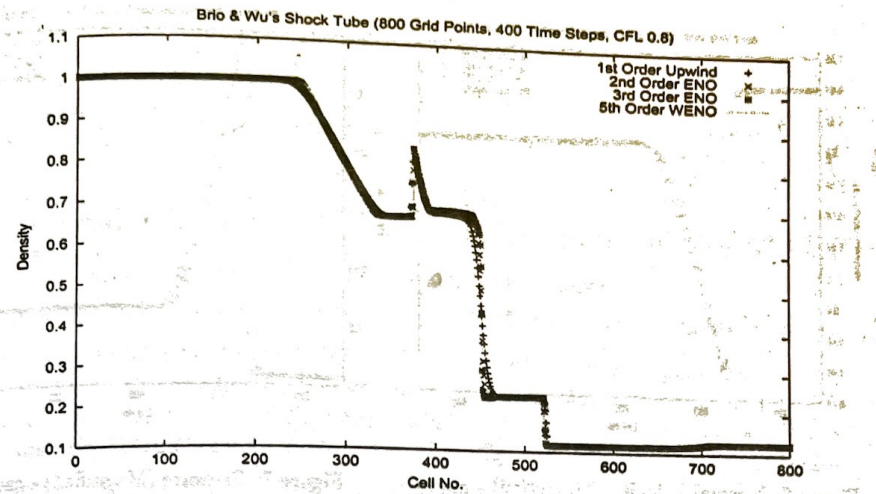


Figure 1: Density - case 1

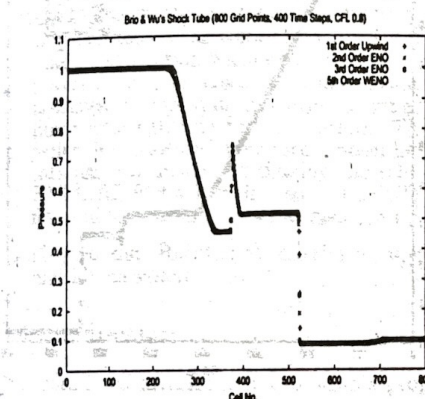


Figure 2: Pressure - case 1

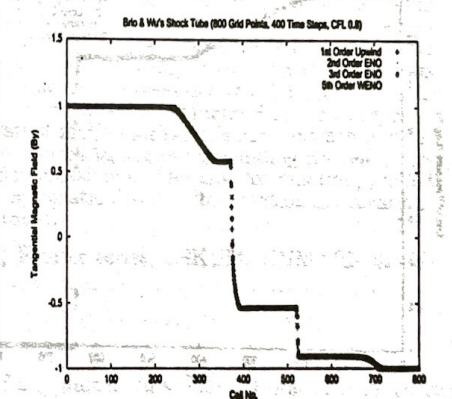


Figure 3: Tangential Magnetic Field - case 1

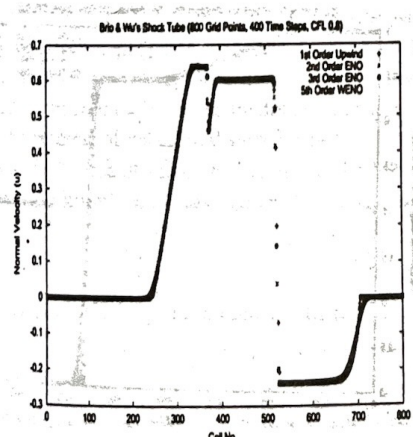


Figure 4: Normal Velocity - case 1

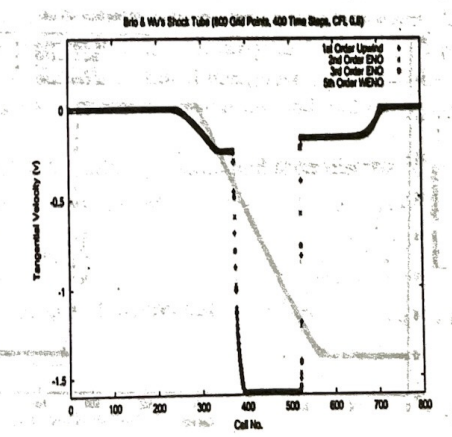


Figure 5: Tangential Velocity - case 1

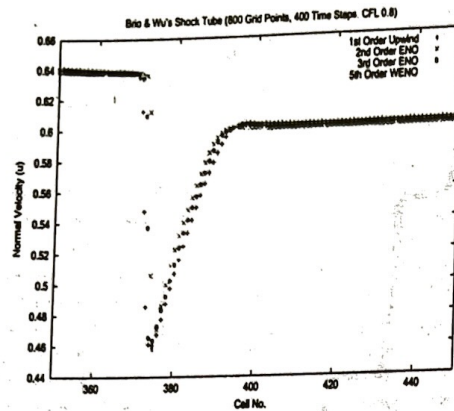


Figure 6: Normal Velocity (Magnified) - case 1

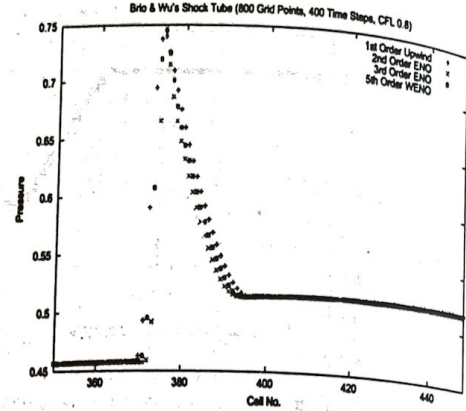


Figure 7: Pressure (Magnified) - case 1

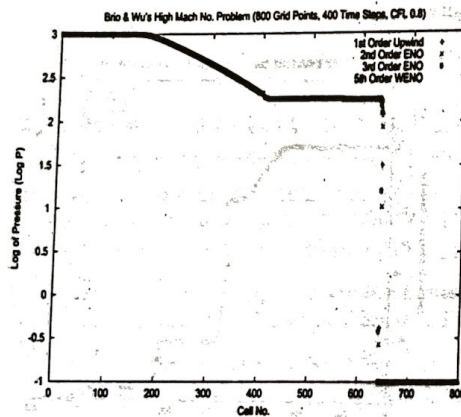


Figure 8: Log of pressure - case 2

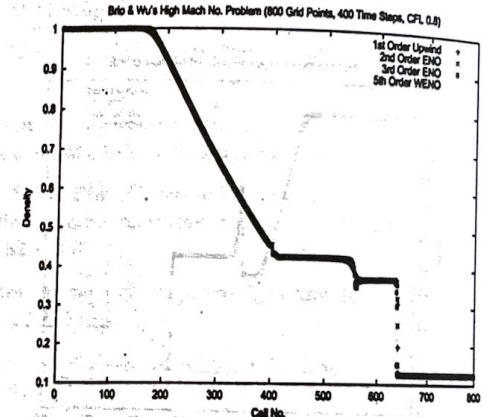


Figure 9: Density - case 2

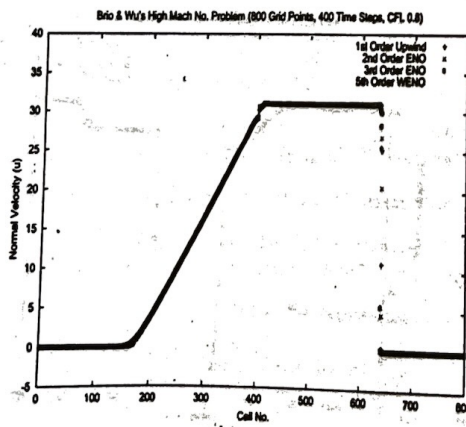


Figure 10: Normal Velocity - case 2

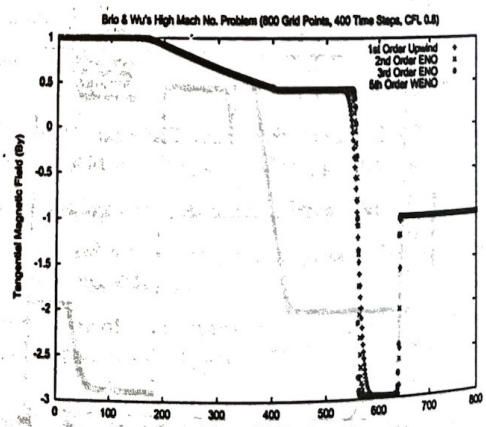


Figure 11: Tangential Magnetic Field - case 2



*Proceedings
of the
8th Annual CFD Symposium*

CFD Division of AeSI

11th - 13th August 2005

S.R. Valluri Auditorium
National Aerospace Laboratories
Bangalore - 560 017